Polymer Nanostructures

DOI: 10.1002/ange.200703348

Direct Synthesis of Anisotropic Polymer Nanoparticles**

Tao He, Dave J. Adams, Michael F. Butler, Chert Tse Yeoh, Andrew I. Cooper, and Steven P. Rannard**

The production of materials with control over structure on the nanometer scale is of fundamental importance in science and technology. Here we demonstrate the direct synthesis of polymer nanoparticles with targeted shapes in the size range <100 nm, without requiring functional groups to induce self-assembly. This one-pot route can be scaled up since it uses conventional polymerization techniques and reagents at high concentrations to synthesize both spherical and anisotropic "dumbbell-like" nanoparticles directly from simple vinyl monomers.

There are few nonbiological examples of the direct chemical synthesis of complex, nonspherical organic nanostructures.[1] There has been much interest in the *indirect* formation of nanostructures by cooperative molecular assembly of presynthesized macromolecular building blocks. For example, certain amphiphilic block copolymers self-assemble to form block copolymer micelles or vesicles, which may then be chemically transformed into static, shell-cross-linked spherical[2–7] and toroidal[8] nanostructures (typical diameters <100 nm).[9] Alternatively, linear triblock rod-coil amphiphiles with incompatible blocks may form mushroom-shaped aggregates with dimensions of 8 nm by 2 nm which can stack to generate supramolecular plate and tape structures.[10]

Controlled radical polymerization[11–13] has been used to produce linear block copolymers which self-assemble into nanomaterials. Recently, conventional[14–16] and controlled[17–20] radical polymerization was also used to produce soluble, high molar mass, branched homopolymers in single-pot procedures. In this study, we synthesize complex polymer nanostructures using a one-pot atom-transfer radical polymerization[11] (ATRP) approach, avoiding separate self-assembly and chemical-fixation steps.

Initially, we produced simple linear AB amphiphilic diblock copolymers (see the Supporting Information), which do not self-assemble to form organic nanoparticles, using aqueous phase ATRP.[21,22] Well-defined branched block-copolymer nanoparticles were then synthesized by a controlled branching strategy (Figure 1). In the presence of a bifunctional monomer, ethyleneglycoldimethacrylate (EGDMA **4**; 0.9:1 ratio relative to initiator **1**), the growing hydrophobic poly(*n*BuMA) blocks were able to branch and form chemical bonds between other growing poly(*n*BuMA) blocks, hence building a structure composed of covalently linked copolymer chains (Figure 1). The ratio of branching bifunctional monomer units to the growing macromolecule chain is restricted to less than one branched monomer per chain, and thus the formation of a typical macromolecular network is inhibited[16] and discrete soluble molecular species are formed (Figure 1B), in a similar fashion to star polymers of lower molar mass which have been formed by the "arm first" ATRP method.[23–26] Dialysis was used to remove the THF along with any residual monomer, initiator, or catalyst and to generate a clear, homogeneous aqueous solution in which the internal hydrophobic branched poly(*n*BuMA) blocks form a collapsed nanoparticle core (Figure 1B). When more EGDMA was used (1.3:1 ratio of **4**/**1**), microgel fractions formed and the resultant aqueous solutions were cloudy rather than clear after dialysis.

TEM investigation of the dialyzed sample revealed individual, spherical nanoparticles with a mean particle diameter of 43.2 nm (Figure 2B; see Figure S9 in the Supporting Information). These particles are generally similar in size to those reported for shell-cross-linked micelles,[2–7] but, importantly, they have been synthesized in a single reaction sequence rather than by assembly and cross-linking of preformed polymers. The polymerizations were conducted at 35% w/v solids as opposed to the typically low concentrations used for the formation of shell-cross-linked micelles.[2–7] Analysis of the aqueous solutions formed after dialysis by dynamic light scattering (DLS) (Figure 2C) showed a narrowed size distribution with a *z*-average particle diameter of 32.5 nm (polydispersity index (PDI) = 0.097). This diameter is somewhat smaller than the mean diameter estimated by AFM analysis (40–50 nm; see the Supporting Information) and by TEM (43.2 nm; see Figure S10 in the Supporting Information), probably because of spreading on the TEM/mica surfaces. The overall size distributions are, however, similar (see Figure 2C,D). By contrast, irregular filmlike structures with large (>300 nm) aggregates were observed after solvent evaporation for the simple linear diblock copolymers (Figure 2A; see Figure S8 in the Supporting Information). There was no evidence for well-defined, self-assembled nanoparticles.

Our chemical synthesis strategy allows the rational design and manipulation of nanoparticle size by varying the block lengths. A systematic increase in average *z*-average particle

[*] T. He, C. T. Yeoh, Prof. A. I. Cooper, Prof. S. P. Rannard
Department of Chemistry, University of Liverpool
Crown Street, Liverpool (UK)
Fax: (+44) 15-1794-2304
E-mail: aicooper@liv.ac.uk
srannard@liv.ac.uk
D. J. Adams, M. F. Butler
Unilever Corporate Research
Colworth, Sharnbrook, Bedfordshire, MK44 1LQ (UK)

[**] The authors gratefully acknowledge Unilever Corporate Research and EPSRC for funding (EP/C511794/1). S.R. acknowledges the Royal Society for an Industrial Fellowship.

Supporting information for this article is available on the WWW under http://www.angewandte.org or from the author.

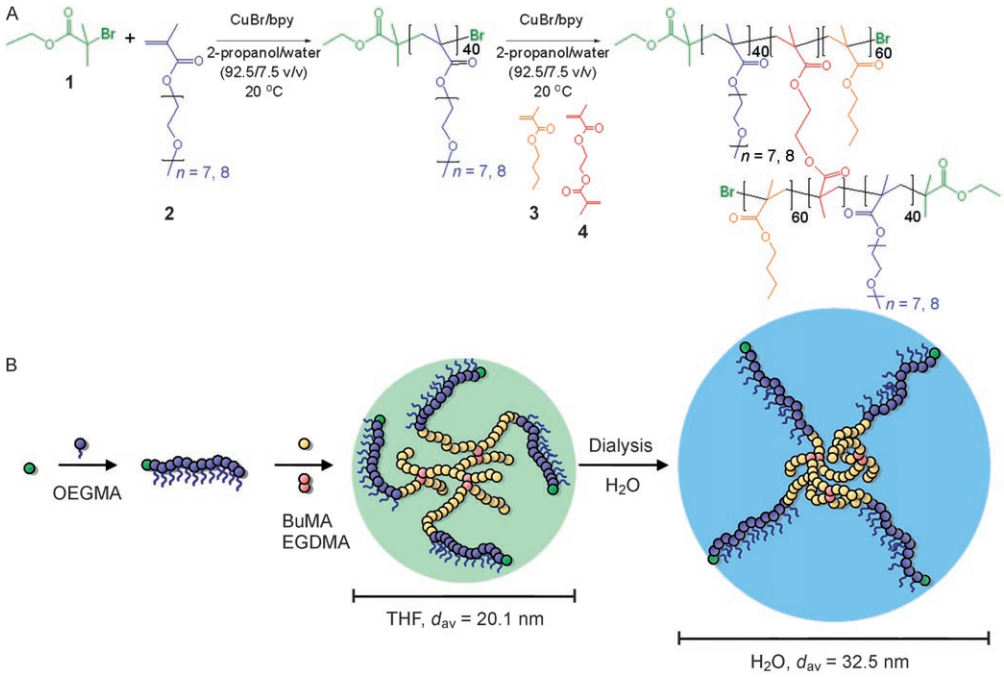

Figure 1. A) Synthesis of AB branched block copolymer by ATRP with introduction of the dimethacrylate brancher **4**. B) Schematic of branched copolymer structure in THF and collapse of the poly(*n*BuMA) branched core in water. Diameters refer to *z*-average values determined by dynamic light scattering. bpy = 2,2′-bipyridine.

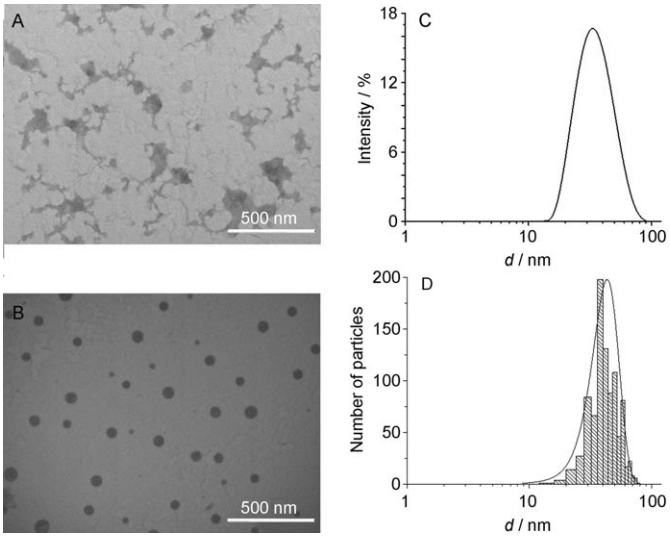

Figure 2. A) TEM image of film formed by deposition of a heterogeneous suspension of phase-separated linear poly(OEGMA)-*b*-poly(*n*BuMA) diblock copolymer in water. B) TEM image of branched block copolymer nanoparticles deposited from a homogeneous aqueous solution. C) DLS data for branched block copolymer nanoparticles in water; *z*-average diameter = 32.5 nm. D) Histogram showing particle size distribution for these particles by TEM analysis (900 particles measured; mean diameter = 43.2 nm; standard deviation = 10.6 nm).

diameter determined by DLS after dialysis was observed for a series of three AB branched block copolymers (31.2 nm, 32.5 nm, 37.7 nm) with poly(OEGMA)/poly(*n*BuMA) block ratios of 40:40, 40:60, and 40:80 repeat units, respectively.

In contrast to more established polymerization routes such as emulsion polymerization, which produce spherical particles, this method may be extended to more complex nanoscale architectures. For example, we synthesized anisotropic dumbbell structures with targeted shapes at the multinanometer scale in a one-pot reaction (Figure 3). The one-pot living polymerization was carried out exactly as before (40:60 OEGMA/*n*BuMA) except for the addition of the bifunctional initiator **5** in the initial poly(OEGMA) growth stage (Figure 3A). This combined initiator system (20:80 **5**/**1**) generates a mixture of linear poly(OEGMA) chains where the number-average molecular weight of the "bifunctional" polymer derived from **5** (roughly 80 OEGMA units) is approximately twice that of the polymer derived from initiator **1** (roughly 40 units). Subsequent addition of *n*BuMA and EGDMA produces a mixture of branched AB and ABA block copolymers having poly(*n*BuMA) segments of identical length. The ABA copolymers generated from initiator **5** have two propagating branching chain ends, which are designed to form a statistically governed number of bridging chains between the cores of the growing spherical nanoparticles, hence forming dumbbell-like nanostructures (Figure 3B).

The sample was dialyzed as before to form a stable dispersion of polymer nanoparticles in water. TEM investigations (Figure 4; see Figure S12 in the Supporting Information) revealed structures very different from those observed for particles prepared in the absence of initiator **5**. Of the 900 particles measured by TEM, 56% were found to have elongated, dumbbell-like morphologies resembling two conjoined spheres. The degree of elongation and separation between the conjoined spheres was found to vary (see Figure 4D and Figure S15 in the Supporting Information as well as the associated discussion). Structures of this type were never observed for the branched AB block copolymer formed using initiator **1** alone; equivalent TEM analysis showed exclusively spherical structures (Figure 2D). Cryogenic TEM analysis of a frozen aqueous solution of the mixed AB/ABA branched copolymers also showed the presence of anisotropic particles. The nanoparticles observed using cryogenic TEM (see Figure S13 in the Supporting Information) were more oblate and exhibited less structural definition, most likely because of aqueous solvation of the poly(OEGMA) chains.

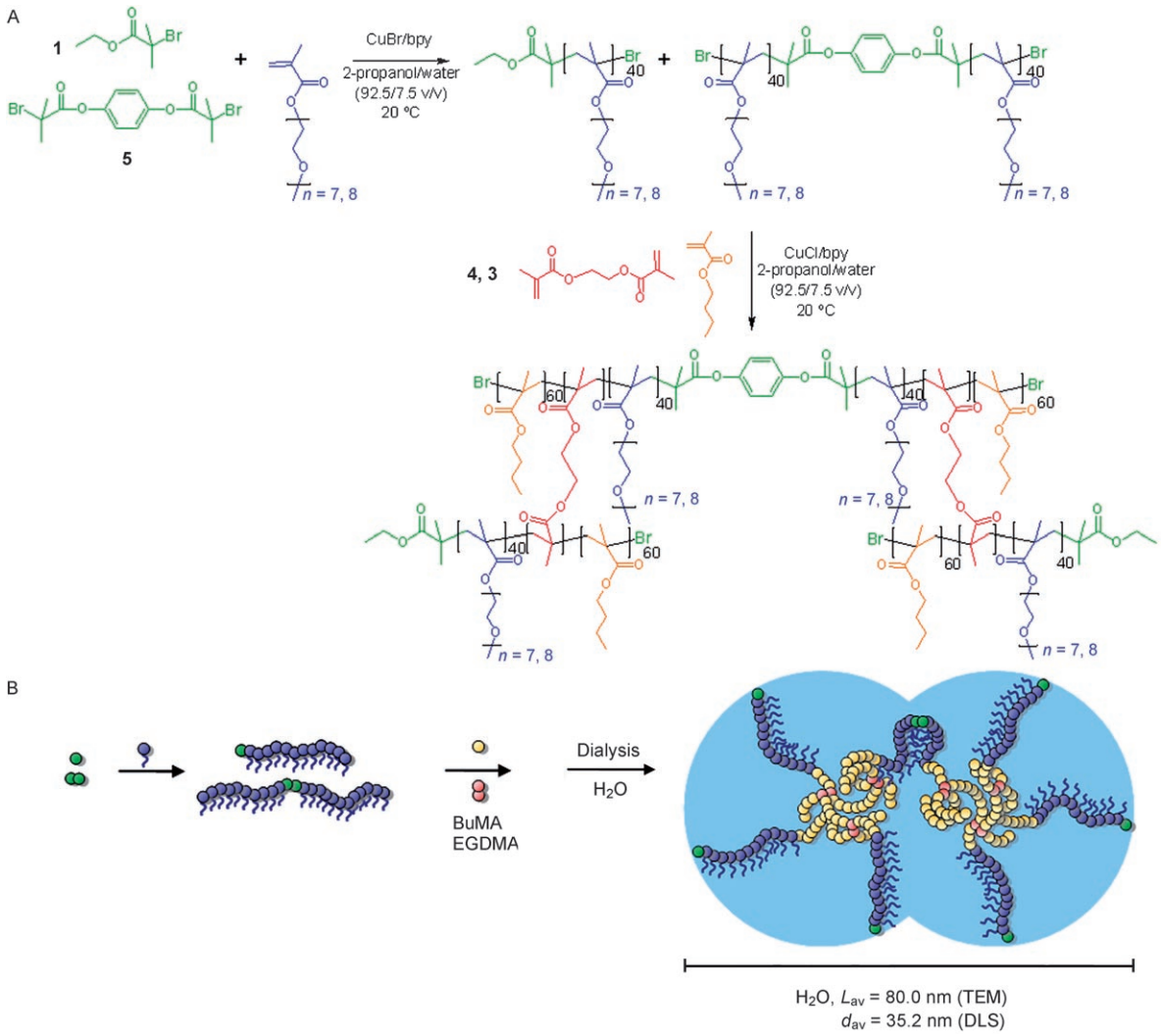

Figure 3. A) Targeted synthesis of dumbbell-like polymer nanoparticles by introduction of the difunctional ATRP initiator **5**. B) Schematic representation of a polymer dumbbell nanostructure showing two poly(OEGMA)-protected poly(*n*BuMA) cores covalently connected by a difunctional poly(OEGMA) chain derived from initiator **5**. It should be noted that the DLS diameter is a spherical average and that this is a poor estimate for anisotropic structures.

These cryoscopic measurements in situ rule out complex association phenomena that can occur during drying as a mechanism for formation of the structures. While inherently anisotropic polymer colloids have been prepared before,[27] we believe that this is the first example of a direct, targeted synthesis of such materials.

There are two nonexclusive mechanisms by which the dumbbells could be formed: coupling of preformed spheres or a concerted growth process. The size distribution for the spherical particles was found to be very similar to the size distribution for the component halves of the dumbbells (see Figure S15 in the Supporting Information), although these statistics would be expected for both stepwise and concerted processes. Preliminary TEM studies of the growth mechanism suggest that some nascent dumbbell structures (< 20 nm in length) are formed at quite low *n*BuMA conversions (<30 %). This implies that the process is, at least in part, a concerted growth mechanism. These same studies also suggest, however, that the proportion of dumbbell structures increases with *n*BuMA conversion, making it likely that particle–particle coupling plays a role at higher monomer conversions. The importance of phase separation between the poly(OEGMA) and poly(*n*BuMA) blocks in forming the well-defined dumbbell shape is as yet unclear, although it should be noted that less structural definition was apparent for in situ cryo-TEM experiments (see Figure S13 in the Supporting Information).

The schemes presented in Figure 1 B and Figure 3 B are very simplistic. First, the structures are composed of many more covalently linked chains. A spherical poly(OEGMA)$_{40}$-*b*-(poly(*n*BuMA)-*co*-EGDMA)$_{60}$ particle with a diameter of 32.5 nm would have a volume of 17 974 nm^3 and a mass of 1.8×10^{-17} g, if one assumes a nominal bulk density of 1 g cm^{-3}. This would correspond to a covalently linked assembly of more than 600 primary polymer chains and a molar mass per particle of $> 1 \times 10^7$ g mol^{-1}, assuming that the

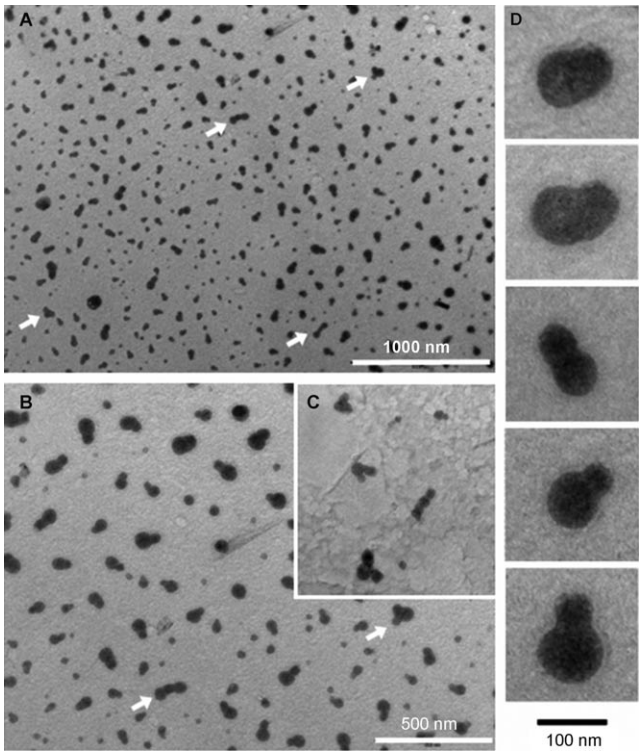

Figure 4. A,B) High- and low-magnification TEM images of dumbbell-like polymer nanoparticles (56% by number) and spherical particles (43%) produced using 20:80 ratio of **5**/**1**. A very small number of higher-order structures (0.5% with three cores, 0.05% with four) were also observed (marked with arrows). C) Inset (same scale as (B)) showing higher-order structures at a ratio of 23:73 **5**/**1**. D) Expansions showing five dumbbell structures formed using 20:80 ratio of **5**/**1** and illustrating the range of topologies in the sample.

molar mass per primary chain is 17000 g mol^{-1}. Given the nature of the DLS measurement, this simple "hard-sphere" comparison and bulk density estimate are crude approximations; nonetheless, it is clear that these particles have very high molar masses and this explains the failed attempts at size-exclusion chromatography (see Supporting Information). A second simplification is that the ABA branched block copolymers derived from **5** may not always grow between two distinct hydrophobic monomer cores, as shown in Figure 3B but might be incorporated into just one core as "loops" or pendant chains. Similarly, multiple ABA chains may link poly(*n*BuMA) core masses. It is also conceivable that the poly(*n*BuMA) cores themselves may spread and bridge, rather than exclusive linking through poly(OEGMA) chains (Figure 3B). However, preliminary experiments show that perfectly cleavable dumbbells may also be synthesized—for example, by building disulfide links into the difunctional initiator, **5**—which supports a model where the dumbbells are *exclusively* linked through these ABA chains. Moreover, there is a total absence of dumbbell structures in the AB branched block copolymer. A further simplification is the representation of clean blocking. Since the *n*BuMA monomer is added at around 85% OEGMA conversion, it is likely that a statistically gradient exists between the poly(OEGMA) and poly(*n*BuMA) blocks, although the unreacted OEGMA (on average 6 units per chain) is in low concentration relative to *n*BuMA (on average 60 units per chain).

These data support unambiguously the formation of unimolecular species rather than physical aggregates. The control over particle structure is imperfect: 43% of spherical species were observed in addition to the target dumbbells. This compares favorably, however, with many self-assembled block copolymer systems where the structure of interest may often be a minority species. A very small number of higher-order structures are also observed (<1%), as would be expected in a statistically governed reaction; both linear and triangular structures consisting of three cores are evident in the distribution (Figure 4A,B marked with arrows). The very small percentage of higher-order structures suggests that steric factors and internal loops (see above) may limit the growth of these structures, which should, on average, have sufficient bifunctional "arms" to bridge much more extensively at a 20:80 ratio of **5**/**1**. The statistical distribution of the nanostructures can be changed by varying the ratio of the mixed initiators, **1** and **5**. Spherical nanostructures are formed exclusively when initiator **1** is used while a 80:20 ratio of initiators **1** and **5** gives mostly (56%) dumbbell nanostructures (Figure 4A,B). At a lower **5**/**1** ratio (10:90) just 16% of dumbbell structures were observed (see Figure S14 in the Supporting Information), the remainder being spherical nanoparticles. By contrast, a 23:77 ratio of **5**/**1** produced mainly higher-order unimolecular structures with three or more linked cores (Figure 4C). Macroscopic formation of a gel, as a result of extended network formation, was observed when the ratio of initiators **5** and **1** was increased to 25:75. The strong sensitivity of the system to the concentration of the difunctional linker **5** is characteristic of a combined step-growth/chain-growth mechanism with substantial increase in molecular weight at higher monomer conversions.[14–17]

In summary, we have demonstrated the direct, targeted, one-pot synthesis of spherical and anisotropic nanostructures on a multigram scale from simple vinyl monomers. Although the basic synthetic strategy is similar to that used to generate star polymers,[22–26] the size and topology of the resulting spherical and dumbbell nanostructures are unprecedented for a one-pot synthesis. These reproducible and simple synthetic techniques offer researchers a design protocol for complex functional nanostructures with specific placement of functionality. More elaborate nanostructures are readily envisaged, for example, by using a derivatized metal or inorganic nanoparticle or biomolecule as a component of the initiating system. Strategies of this type are enabled by the relative ease with which a wide range of molecules and nanostructures have been functionalized with ATRP initiators. The core-shell morphology of these particles suggests applications in encapsulation and controlled release. Anisotropic particles may be useful, for example, as carriers in biological systems where size, chemical functionality, and shape are all important. Our route also presents a number of challenges, for example, in developing strategies to achieve control over the breadth of structures arising from the statistical nature of the branching process. A key challenge will be to develop improved routes with enhanced structural control without sacrificing the simplicity, versatility, and scalability of the approach.

Experimental Section

Full details of the synthetic procedures used to prepared the polymers are included in the Supporting Information. A typical synthetic procedure (for the linear diblock copolymer, poly(OEGMA)$_{40}$-*b*-poly(*n*BuMA)$_{60}$ was as follows: OEGMA (2.04 g, 6.8 mmol), CuBr (24.5 mg, 0.17 mmol), bpy (53.1 mg, 0.34 mmol), and solvent (isopropanol/water (92.5:7.5 v/v; 4.2 mL) were added to a Schlenk flask (50 mL). The reaction mixture was bubbled with nitrogen for 40 min to completely remove the oxygen, before EBriB (ethyl 2-bromoisobutyrate) (25.0 μL, 33.2 mg, 0.17 mmol) was added with a microsyringe. The polymerization was carried out at ambient temperature (≈20 °C) under N_2. In another 50-mL Schlenk flask, CuCl (16.9 mg, 0.17 mmol), byp (53.1 mg, 0.34 mmol), *n*BuMA (1.45 g, 10.2 mmol) and 5.8 mL of the water–alcohol solvent mixture were added, and this mixture was bubbled with N_2 for 1 h. After the conversion of OEGMA reached around 85%, the mixture from the second flask was added into the first flask rapidly using a syringe. The block copolymerization reaction was carried at ambient temperature, and samples were taken periodically from the reaction mixture for ^{1}H NMR analysis. After the consumption of the *n*BuMA monomer had reached around 90%, the polymerization was stopped by adding THF into the reaction mixture and exposing the sample to air.

Received: July 25, 2007
Published online: November 15, 2007

Keywords: atom-transfer polymerization · nanoparticles · polymerization

[1] P. W. K. Rothemund, *Nature* **2006**, *440*, 297 – 302.
[2] K. B. Thurmond, T. Kowalewski, K. L. Wooley, *J. Am. Chem. Soc.* **1996**, *118*, 7239 – 7240.
[3] R. K. O'Reilly, C. J. Hawker, K. L. Wooley, *Chem. Soc. Rev.* **2006**, *35*, 1068 – 1083.
[4] W. Schärtl, *Adv. Mater.* **2000**, *12*, 1899 – 1908.
[5] S. Y. Liu, J. V. M. Weaver, Y. Q. Tang, N. C. Billingham, S. P. Armes, K. Tribe, *Macromolecules* **2002**, *35*, 6121 – 6131.
[6] S. Y. Liu, S. P. Armes, *J. Am. Chem. Soc.* **2001**, *123*, 9910 – 9911.
[7] V. Butun, N. C. Billingham, S. P. Armes, *J. Am. Chem. Soc.* **1998**, *120*, 12135 – 12136.
[8] D. J. Pochan, Z. Y. Chen, H. G. Cui, K. Hales, K. Qi, K. L. Wooley, *Science* **2004**, *306*, 94 – 97.
[9] C. J. Hawker, K. L. Wooley, *Science* **2005**, *309*, 1200 – 1205.
[10] S. I. Stupp, V. LeBonheur, K. Walker, L. S. Li, K. E. Huggins, M. Keser, A. Amstutz, *Science* **1997**, *276*, 384 – 389.
[11] J. S. Wang, K. Matyjaszewski, *J. Am. Chem. Soc.* **1995**, *117*, 5614 – 5615.
[12] D. Benoit, V. Chaplinski, R. Braslau, C. J. Hawker, *J. Am. Chem. Soc.* **1999**, *121*, 3904 – 3920.
[13] J. Chiefari, Y. K. Chong, F. Ercole, J. Krstina, J. Jeffery, T. P. T. Le, R. T. A. Mayadunne, G. F. Meijs, C. L. Moad, G. Moad, E. Rizzardo, S. H. Thang, *Macromolecules* **1998**, *31*, 5559 – 5562.
[14] S. Graham, P. A. G. Cormack, D. C. Sherrington, *Macromolecules* **2005**, *38*, 86 – 90.
[15] F. Isaure, P. A. G. Cormack, D. C. Sherrington, *Macromolecules* **2004**, *37*, 2096 – 2105.
[16] N. O'Brien, A. McKee, D. C. Sherrington, A. T. Slark, A. Titterton, *Polymer* **2000**, *41*, 6027 – 6031.
[17] F. Isaure, P. A. G. Cormack, S. Graham, D. C. Sherrington, S. P. Armes, V. Bütün, *Chem. Commun.* **2004**, 1138 – 1139.
[18] B. L. Liu, A. Kazlauciunas, J. T. Guthrie, S. Perrier, *Macromolecules* **2005**, *38*, 2131 – 2136.
[19] V. Butun, I. Bannister, N. C. Billingham, D. C. Sherrington, S. P. Armes, *Macromolecules* **2005**, *38*, 4977 – 4982.
[20] I. Bannister, N. C. Billingham, S. P. Armes, S. P. Rannard, P. Findlay, *Macromolecules* **2006**, *39*, 7483 – 7492.
[21] X. S. Wang, S. P. Armes, *Macromolecules* **2000**, *33*, 6640 – 6647.
[22] S. McDonald, S. P. Rannard, *Macromolecules* **2001**, *34*, 8600 – 8602.
[23] J. Xia, X. Zhuang, K. Matyjaszewski, *Macromolecules* **1999**, *32*, 4482 – 4484.
[24] K.-Y. Baek, M. Kamigaito, M. Sawamoto, *Macromolecules* **2001**, *34*, 215 – 221.
[25] X. Zhang, J. Xia, K. Matyjaszewski, *Macromolecules* **2000**, *33*, 2340 – 2345.
[26] H. Gao, K. Matyjaszewski, *Macromolecules* **2006**, *39*, 3154 – 3160.
[27] Z. Q. Yang, W. T. S. Huck, S. M. Clarke, A. R. Tajbakhsh, E. M. Terentjev, *Nat. Mater.* **2005**, *4*, 486 – 490.